Non-volatile electrically programmable integrated photonics with 5-bit operation based on phase-change material Sb_2S_3

Rui Chen[1,*], Zhuoran Fang[1], Christopher Perez[3], Forrest Miller[1], Khushboo Kumari[1], Abhi Saxena[1], Jiajiu Zheng[1], Sarah J. Geiger[4], Kenneth E. Goodson[3], Arka Majumdar[1,2,*]

[1] *Department of Electrical and Computer Engineering, University of Washington, Seattle, WA 98195, USA*
[2] *Department of Physics, University of Washington, Seattle, WA 98195, USA*
[3] *Department of Mechanical Engineering, Stanford University, Stanford, CA 94305, United States*
[4] *The Charles Stark Draper Laboratory, Cambridge, MA 02139, USA*
[5] *Department of Electrical Engineering, Stanford University, CA 94305, USA*
[*] charey@uw.edu, *arka@uw.edu*

Abstract: We report a hybrid phase-change mateial Sb_2S_3-silicon photonic tunable directional coupler, which exhibits low insertion loss (< 1.0 dB), large extinction ratio (> 10 dB), high endurance (> 1,600 switching events), and 32 operation levels.

Phase-change materials (PCMs) have been used for tunable integrated photonic devices based on the optically/electrically different phases (amorphous (a) and crystalline (c) phase) [1–3]. Notably, the reversible phase transition in PCMs is non-volatile under ambient environments. Therefore, by switching PCMs' material phase, the phase/amplitude of light can be changed in a truly "set-and-forget" fashion, requiring zero static power supply.

Traditional PCMs, such as GST, were only optimized for electronic memory applications, but not for photonics. In fact, GST exhibits high absorption loss in the visible and near IR wavelength range. Recently, wide-bandgap phase-change materials, such as Sb_2Se_3 and Sb_2S_3 [4,5], show a promising path for low-loss PCM-based integrated photonic devices. These wide-bandgap PCMs exhibit almost zero absorption in the telecommunication wavelengths (1310 nm and 1550 nm), qualifying them for phase-only modulation in both integrated photonics [6,7]. However, current demonstrations mostly rely on the fast laser pulses to reversibly switch Sb_2S_3 [5,8]. While electrical control is a necessity towards more feasible and larger-scale PIC systems, current electrically controlled Sb_2S_3 works are limited by fast device degradation and very few cycles (< 10 cycles) [5].

In this work, we demonstrate the electrical switching of Sb_2S_3-silicon photonic device (a tunable beamsplitter) with high endurance (> 1,600 switching events). The integrated photonic device shows a low insertion loss (< 1.0 dB) and large extinction ratio (> 10 dB). Interestingly, we observed a stepwise multi-level performance by sending the same electrical pulses multiple times. Furthermore, by adding dynamic pulse control, we achieve 5-bit (32 levels) operations with 0.50 ± 0.16 dB contrast per step. Our demonstration is a crucial step toward energy-efficient and large-scale optical trimming, microwave photonics, and optical neural networks.

We designed and fabricated a compact asymmetric directional coupler with a coupling length of 79 μm. As shown in Fig. 1a, two waveguides of the coupler were designed to have different widths. The narrower waveguide (409 nm wide, cladded with Sb_2S_3) was sputtered with 20-nm-thick Sb_2S_3, and designed to phase match to the wider waveguide (450 nm wide, bare silicon waveguide) for c-Sb_2S_3[9]. As such, the input light could completely couple to the cross port in one coupling length. Once Sb_2S_3 is switched to the amorphous state, the effective index of the hybrid waveguide changes while the bare waveguide remains the same. The resulting phase-mismatch changes the coupling length and amplitude and leads to a complete bar state after optimizing the gap (420 nm). We note that the footprint of the coupler can be potentially reduced (~ 34 μm) by depositing a thicker (50 nm) Sb_2S_3 to provide stronger refractive index contrast.

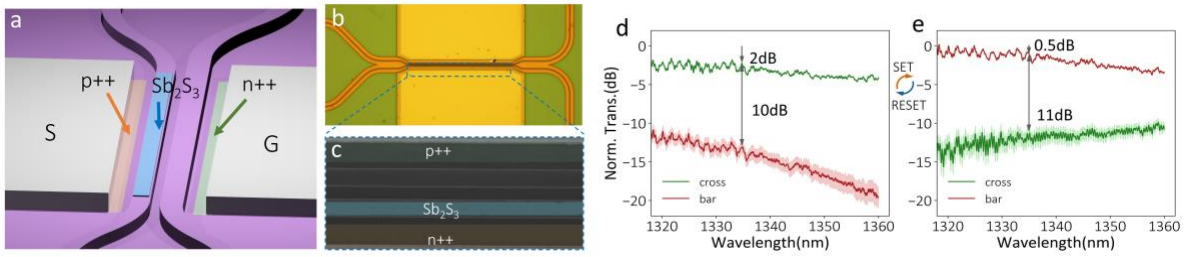

Fig. 1. An electrically switchable, non-volatile asymmetric directional coupler using Sb_2S_3-silicon hybrid waveguide. (a) Schematic, (b) optical and (c) SEM images of the tunable directional coupler. (d, e) Transmission spectra at bar and cross ports for (d) a-Sb_2S_3 (RESET: three 9.6 V, 500 ns pulses) and (e) c-Sb2S3 (SET: three 2.7 V, 200 ms pulses). The result was averaged over five measurements, and the shaded region indicates the standard deviation.

Figs. 1d and 1e show the transmission spectra for a- and c-Sb_2S_3, respectively. The Sb_2S_3 film was switched with three 9.6 V, 500 ns RESET, and 2.7 V, 200 ms SET pulses, respectively. The insertion losses are 2 dB (0.5 dB), and the extinction ratios are around 10 dB (11 dB) for a (c)-Sb_2S_3). The unusually high insertion loss when the Sb_2S_3 is in the amorphous state is likely because grating coupler fabrication imperfection. We estimated actual Sb_2S_3 loss by putting Sb_2S_3 thin films in high-Q ring resonators, and the estimated loss is three times higher than blanket ellipsometry result, which could be attributed to crystallite scattering loss. We implement the measured loss and estimated this device's insertion loss to be ~0.1 dB (0.9 dB) for a(c)-Sb_2S_3.

In Figs. 2a and 2b, we show 1,600 switching events for the device. Limited by our measurement setup, we separately measured the cross (Fig. 2a) and bar ports (Fig. 2b). The higher insertion loss (~1 dB) at around event 500 was due to optical fiber misalignment. We note that little performance degradation occurred in the end, and hence, this device is not limited to the tested cyclability. Surprisingly, our Sb_2S_3 integrated structures show a stepwise multilevel operation, and the number of operation levels reached 32 levels with optimized pulses. In Fig. 2c, we show the multi-level transmission at both cross and bar port of an asymmetric directional coupler while sending in RESET 10 V, 550 ns pulses each second to amorphized the Sb_2S_3. We start the experiment with a coarse tune, where unoptimized, identical pulses were sent to partially amorphize the c-Sb_2S_3 device to demonstrate multiple levels. The asymmetric directional coupler was originally in the "cross state" (red region), and after one partial amorphization pulse, it was reconfigured into an intermediate state (orange region), where light comes out from both cross and bar ports. After 6 pulses, a complete "bar state" (green region) was achieved. We repeated this experiment five times and plotted the average transmission levels and the standard deviation. The variation is attributed to the stochastic phase change process using electrical controls[10]. Such multilevel operation is of paramount interest for programmable photonics.

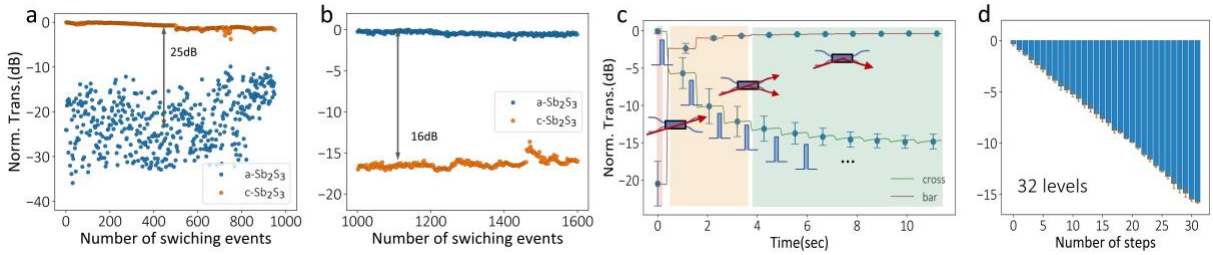

Fig. 2. Cyclability test and multi-level operation for a Sb_2S_3-based asymmetric directional coupler. The device was switched repeatedly by sending in amorphization and crystallization alternatively, and the transmission at a fixed wavelength of 1340 nm was recorded at the (a) cross and (b) bar ports. The blue and orange scatterers represent the normalized transmission when Sb_2S_3 is in the amorphous and crystalline phase, respectively. The device was switched for over 1,600 events with no significant insertion loss and performance degradation. (c) Time trace measurement of the directional coupler when sending in an amorphization pulse (10 V, 550 ns) each second. Cross (bar) transmission is represented by green (red) curves. The result is averaged over 10 experiments and the blue error bar shows the standard deviation. Depending on the pulses sent in, a "bar", "intermediate" and "cross" state can be achieved as indicated by the red, orange, and green regions. (d) Normalized transmission at 1,340 nm at the bar port shows 5-bit operation (32 distinct levels), achieved by dynamically controlling the number, amplitude and duration of pulses sent in (~ 9.75 V, 550 ns). A precise transmission level of 0.50 ± 0.16 dB per step and 32 levels were simultaneously achieved. The only slight difference between the target (0.5 dB per step)and achieved transmission demonstrates an on-demand operation. The orange error bars represent the standard deviation over five experiments.

Acknowledgements

The research is funded by National Science Foundation (NSF-1640986, NSF-2003509), ONR-YIP Award, DARPA-YFA Award, NASA-STTR Award 80NSSC22PA980, and Intel. F.M. is supported by a Draper Fellowship. Part of this work was conducted at the Washington Nanofabrication Facility/ Molecular Analysis Facility, a National Nanotechnology Coordinated Infrastructure (NNCI) site at the University of Washington, with partial support from the National Science Foundation via awards NNCI-1542101 and NNCI-2025489. Part of this work was performed at the Stanford Nano Shared Facilities (SNSF), supported by the National Science Foundation under award ECCS-1542152).

References

1. C. Rios, et al. Nat. Photonics **9**, 725 (2015).
2. J. Zheng, et al. Adv. Mater. **32**, 2001218 (2020).
3. Z. Fang, et al. Nat. Nanotechnol. **17**, 842-848 (2022).
4. M. Delaney, et al. Adv. Funct. Mater. **30**, 2002447 (2020).
5. W. Dong, et al. Adv. Funct. Mater. **29**, 1806181 (2019).
6. Z. Fang, et al. Adv. Opt. Mater. **9**, 2002049 (2021).
7. C. Ríos, et al. PhotoniX **3**, 26(2022).
8. K. Gao, et al. Adv. Funct. Mater. 2103327 (2021).
9. T. Y. Teo, et al. Opt. Mater. Express, OME **12**, 606 (2022).
10. T. Tuma, et al. Nat. Nanotechnol. **11**, 693 (2016).